In situ Raman spectroscopy of low-temperature/high-pressure transformations of H_2O

Yukihiro Yoshimura,[a] Sarah T. Stewart,[b] Ho-kwang Mao, and Russell J. Hemley
Geophysical Laboratory, Carnegie Institution of Washington, Washington, DC 20015

(Received 24 April 2006; accepted 7 March 2007; published online 7 May 2007)

In situ Raman spectra of transformations of H_2O as functions of pressure and temperature have been measured starting from high-density amorphous ice (HDA). Changes above T_x, the crystallization temperature of HDA, were observed. The spectra provide evidence for an abrupt, first-order-like, structural change that appears to be distinct from those associated with the transformation between low-density amorphous ice (LDA) and HDA. In separate experiments, *in situ* Raman spectra of ice XII transformed from HDA have been measured at various *P-T* regions, in order to improve the understanding of the stability limits of ice XII. The spectra of ices VI and XII differ in shape, but the vibrational frequencies are very close in the same *P-T* regimes. A metastable phase of ice found to form within the stability field of ice VI appears to be distinct from ice XII. © *2007 American Institute of Physics*. [DOI: 10.1063/1.2720830]

I. INTRODUCTION

The phase relations of H_2O are complex and include both stable and metastable transitions. Various new phases and transitions continue to be discovered.[1–7] Ice XII found by Lobban *et al.*[2] has a new structure, forms within the stability region of ice V, and contains a mixture of seven- and eight-membered rings.[3] Recent *in situ* x-ray diffraction and Raman spectroscopic studies revealed a structural transition in ice VIII at 10–14 GPa on compression.[5] Salzmann *et al.*[6] found two new proton ordered phases of ice (ices XIII and XIV) that can be prepared by doping proton disordered phases of ices V and XII with HCl. Loerting *et al.*[7] reported that on isothermal compression of high-density amorphous ice (HDA) at 125 K, the material transforms to very high-density amorphous ice[4] (VHDA) at ~1.2 GPa; that is, the stepwise sequence LDA→HDA→VHDA (LDA denotes low-density amorphous ice) takes place.

A liquid-liquid phase transition[8] has been proposed to interpret the well-known anomalous properties of water. According to the hypothesis, supercooled water separates into two phases, low-density liquid water (LDL) to which LDA transforms and high-density liquid water (HDL) to which HDA converts, below a proposed second critical point C_p' at modest pressure and low temperatures. The possibility of a liquid-liquid phase transition together with a second critical point[8,9] is one of the current problems in understanding water.[10] Recently, evidence for a glass transition in HDA has been reported.[11] LDA is believed to show glass transition behavior and transforms to a highly viscous liquid (LDL) when heated to its proposed glass transition temperature [e.g., ~130 K] (Refs. 12 and 13). The identification of the liquid-liquid transition is challenging experimentally because the hypothetical C_p' lies between the homogeneous nucleation temperature[14] (T_H) and the crystallization temperature of amorphous ice (T_X),[15] the so-called "no man's land."[8] In support of this conjecture is the evidence that first-order-like liquid-liquid phase transitions exist in phosphorus[16] and germania,[17] which have open tetrahedral network structures such as liquid water.

The comparison of ice XII and HDA has been of interest.[18–26] Koza *et al.*[18] reported that HDA and ice XII could be produced under similar conditions and decisive conditions favoring ice XII or HDA formation are not clear. They reported that ice XII can form on compression of ice I_h between 77 and ~150 K, and proposed a second regime of metastability of ice XII in order to account for its unexpected formation at low temperatures. Subsequently, Kohl *et al.*[21] described conditions for transforming HDA to ice XII and other high-pressure phases (ice IV or VI) using controlled uniaxial compression of hexagonal ice I_h.

The richness of the ice phase diagram at these modest pressures is an excellent demonstration of the versatility of hydrogen bonding structures built from the water molecule. This flexibility allows very close competition of phases that may be kinetically stabilized in the same *P-T* region depending on the path of formation. *In situ* measurements of ice formed at modest pressures and low temperatures are therefore essential for identifying these phases and understanding their stability and properties. The study of metastable transitions especially requires careful consideration of sample history and following well-defined *P-T* paths along with these *in situ* measurements.

Here we report *in situ* Raman measurements and optical observations of H_2O as functions of pressure and temperature. We compared the results for metastable phases of H_2O obtained on various *P-T* paths starting with HDA. The results provide new insight into the metastable transformations

[a]Author to whom correspondence should be addressed. Present address: Department of Applied Chemistry, National Defense Academy, 1-10-20 Hashirimizu, Yokosuka, Kanagawa 239-8686, Japan. FAX: (+) 81 46 844 5901. Electronic mail: muki@nda.ac.jp
[b]Present address: Department of Earth and Planetary Science, Harvard University, 20 Oxford St., Cambridge, Massachusetts 02138.

of H_2O. The remainder of the paper is organized as follows. In Sec. II, we summarize the experimental methods. Sec. III presents the various metastable transitions observed starting with HDA. We discuss our results in the context of the phase behavior of amorphous ice phases together with a proposed liquid-liquid phase transition hypothesis and the relationships between recently observed metastable phases of ice in Sec. IV. The conclusions of the study are summarized in Sec. V.

II. EXPERIMENTAL METHODS

Raman spectroscopy supplemented by optical microscopy at high pressures and low temperatures were performed using diamond anvil cell techniques analogous to the previous *in situ* observations of the I_h-HDA transition.[1] Doubly distilled and de-ionized water and ruby chips were held in Mao-Bell diamond cells using a stainless steel gasket. The cryostat was equipped with windows, which allow *in situ* optical spectroscopy (e.g., Raman and ruby fluorescence measurements) without changing the *P-T* conditions on the sample. The pressure was controlled from the outside by a mechanical change in the load on lever arms of the cell. To determine the pressure, we used the pressure dependence on the R_1 fluorescence line of ruby.[27,28] At the lowest pressures (e.g., below 0.1–0.2 GPa), it was difficult to obtain precise transition pressure values due to insensitivity of the ruby fluorescence. At these conditions, the sample pressure was determined from the change in load on the lever arm. The diamond-anvil cell equipped with two heaters and thermocouples was cooled by continuous-flow liquid nitrogen. The temperature was measured to within ±1 K. Raman spectra were collected by a single-grating ISA HR-460 spectrometer equipped with a charge-coupled device detector. The 514.5 nm line of an argon-ion laser was typically used.

III. RESULTS

A. Metastable transitions of HDA

The *P-T* paths followed are shown schematically on the equilibrium phase diagram of H_2O in Fig. 1. All paths involved first the formation of HDA by compressing ice I_h above at least 1.5 GPa at 77 K. These changes were accompanied by major changes in the texture of the sample due to the large volume collapse associated with the transition (Fig. 2).[1] Path 1 involved forming HDA by compressing ice I_h up to ~1.5 GPa at 77 K.[29] HDA was then decompressed to ~0.6 GPa while keeping the temperature at ~77 K (path 2) and subsequently warmed slowly at 2.5 K/min to ~145 K (path 3). Again, at a constant temperature of ~145 K HDA was decompressed to near ambient pressure and subsequently recompressed to ~0.4 GPa to examine the reversibility of the transformation (path 4). We measured the Raman spectra at as high a temperature as possible above T_x.

Measurements were performed along paths 3 and 4 to examine transitions from HDA. These *in situ* Raman spectra with changing pressure and temperature are shown in Fig. 3. We note first that the relative intensity of the band centered at ~3500 cm^{-1} increases significantly from 80 to 145 K at 0.6 GPa, and the spectrum begins to resemble that of supercooled water. In fact, the spectrum of supercooled water under pressure increases in intensity in this frequency region, and its intensity decreases as the temperature is lowered.[30] In this *P-T* range (0.6 GPa and 145 K), the system is close to T_x of HDA.

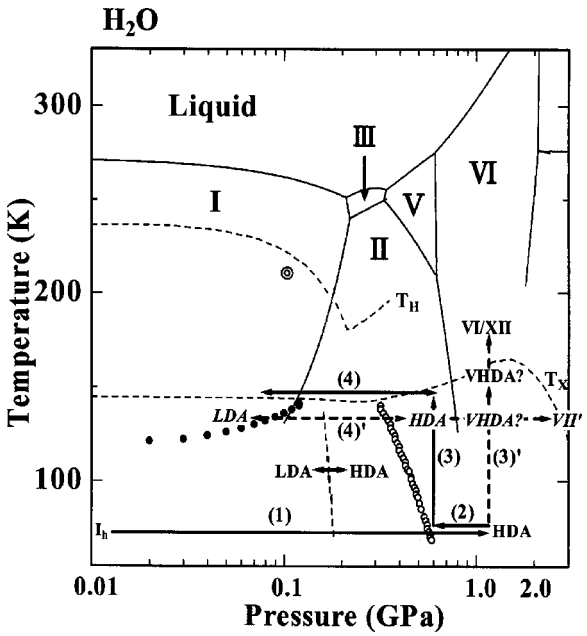

FIG. 1. Experimental paths followed in the present study shown on the equilibrium phase diagram of H_2O. Numbers 3 and 4 correspond to the *P-T* conditions of the Raman results shown in Fig. 3. (3)′ and (4)′ correspond to the *P-T* conditions of the Raman results shown in Figs. 7 and 5, respectively. Open circles shows pressure-induced transitions from LDA to HDA and closed circles shows decompression-induced transitions from HDA to LDA published in Ref. 15. ◎ shows the location of the second critical point of water proposed by Mishima and Stanley (Ref. 59).

Notable changes in the Raman line shapes of the initial phase were observed with decreasing pressure from 0.6 to 0.4 GPa in path 4 (Fig. 3), i.e., when crossing the T_x

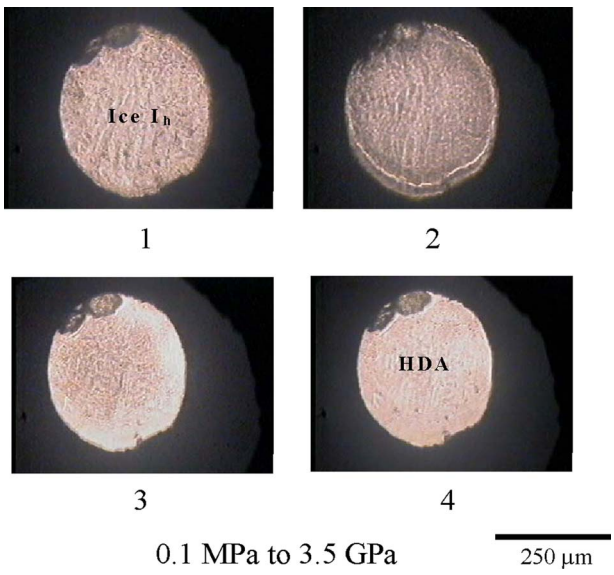

FIG. 2. (Color online) Photomicrographs showing the transformation of ice I_h to HDA from near 0.1 MPa to ~3.5 GPa. The gray areas in images 2 and 3 show the mixed phase parts of the sample during the course of the transition.

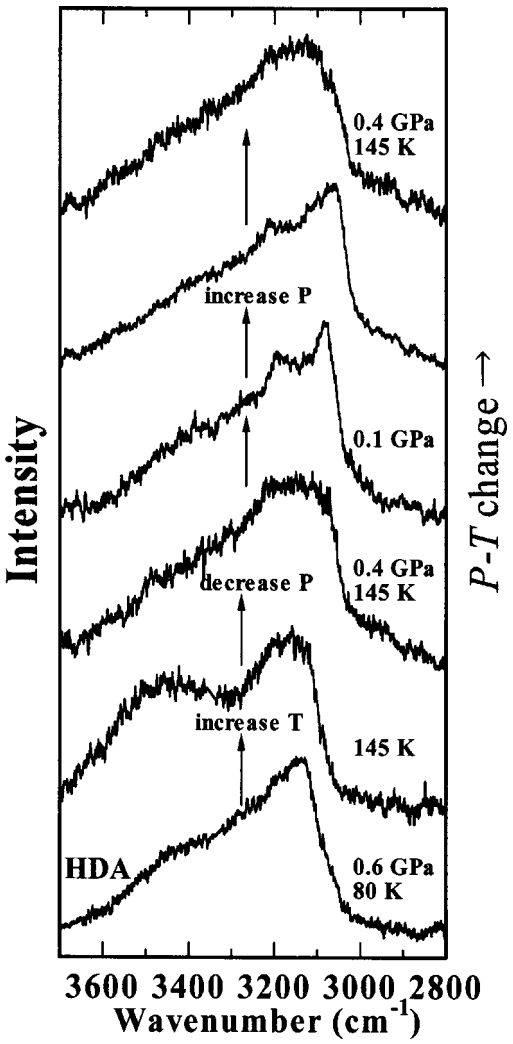

FIG. 3. HDA probed by *in situ* Raman OH stretching spectra as functions of pressure and temperature.

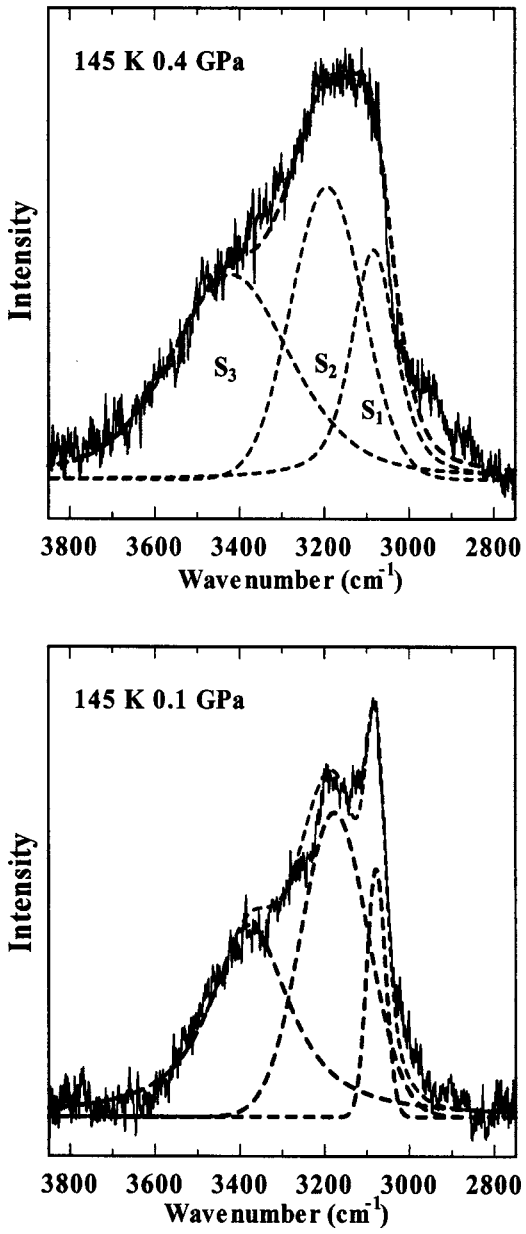

FIG. 4. Representative band component analyses of Raman OH stretching bands following the pressure-induced reversible transition between the two phases at ~145 K. Dotted lines represent deconvoluted peaks.

line. The intensity of the 3500 cm^{-1} band decreased and increased width of the 3150 cm^{-1} band on decompression suggest partial recovery of a structure with stronger hydrogen bonds. The *P-T* conditions explored are very close to the reported T_g of HDA.[11] Upon further decompression, the spectrum changed dramatically near ~0.1 GPa. As discussed below, we believe this change is due to the formation of a phase that is distinct from LDA. The measurements show the transition is reversible (i.e., changing the pressure results in a reversible transformation between them), and it appears rapid and sharp (at 0.1–0.3 GPa). We found no evidence for an intermediate phase.

OH stretching bands of these phases are broad and complex, reflecting Fermi resonance couplings and a mixture of symmetric and antisymmetric OH stretching vibrations. Although they present difficulties for quantitative interpretation, the higher frequency components are generally attributed to the weaker hydrogen-bonded molecules, whereas the lower frequency components are associated with stronger hydrogen bonding. The spectra can be represented by three mixed Gaussian-Lorentzian curves (Fig. 4). On decompression, the intensity of the first Raman band (S_1) increases significantly together with narrowing. These changes in pressure dependence clearly reflect different structural changes on compression.

Additional experiments were performed about 5 K below the above experiments (path 4′) to examine the relationship of the above results to the LDA-HDA transition, which can occur at similar *P-T* conditions.[11] As shown in Fig. 5, the spectral changes observed in these runs differ significantly from those in Fig. 3. With decreasing pressure, a band at ~3100 cm^{-1} appears and begins to grow at the expense of the bands of HDA. It is remarkable that a mixture of LDA and HDA spectra was obtained (e.g., at 0.3–0.1 GPa) upon decompression. The important finding here is that HDA changed to LDA to give coexistence of the two phases, with no evidence for intermediate structures, as the pressure was

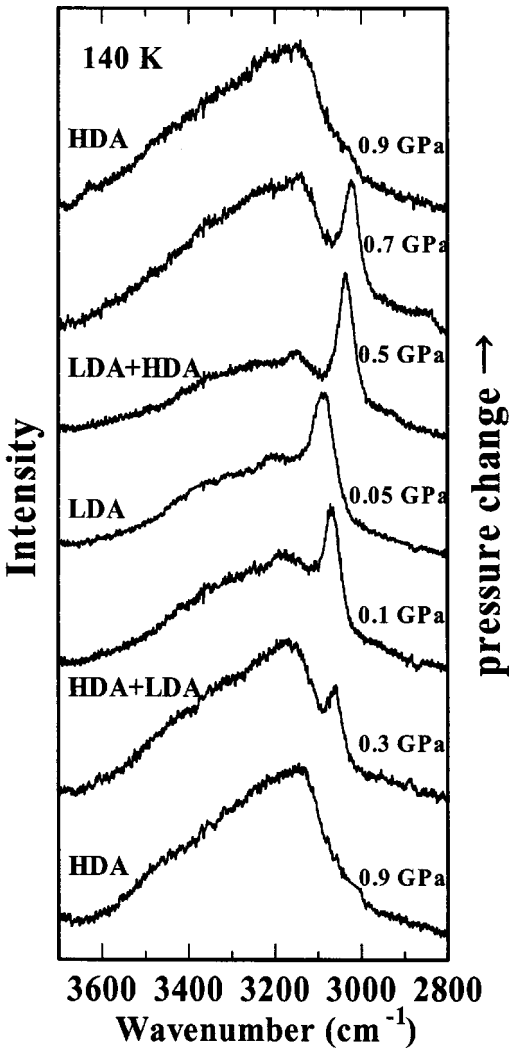

FIG. 5. *In situ* Raman spectra in the OH stretching region measured during the pressure-induced reversible transition between LDA and HDA at ~140 K (path 4′). We prepared the LDA and/or HDA samples by methods described in the literature. (Refs. 29 and 31). HDA transformed to LDA completely at ~0.1 GPa, whereas the LDA changed to HDA at 0.8–0.9 GPa in our measurements.

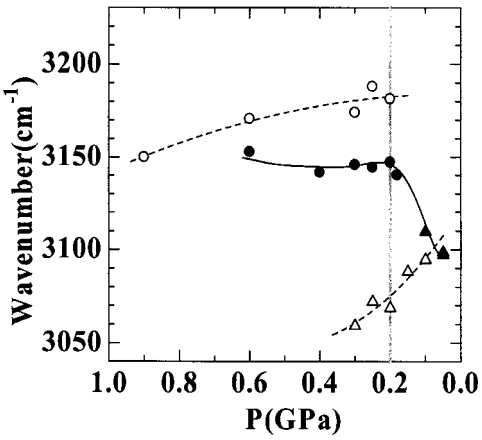

FIG. 6. Comparison of Raman frequency changes between Figs. 3 and 5 upon decompression: HDA (○) and LDA (△) in Fig. 5, and the corresponding peaks (●) and (▲) in Fig. 3. The vertical thick line shows the estimated transition point between the two phases. The solid and dashed curves are guides to the eye.

gradually reduced. On repressurizing the sample, LDA began to transform to HDA around 0.15 GPa. Again LDA changed to HDA, showing the coexistence of LDA and HDA.

Figure 6 compares the frequency shifts in the two runs, where the results for the strongest peak of each spectrum in Figs. 3 and 5 on decompression are plotted. Concordance with the spectral changes, the frequency change at the LDA-HDA transition shows a transition region (0.2–0.3 GPa), whereas the other does not. Thus, the structural change observed in path 4 seems to be distinct from that associated with the transformation between LDA and HDA.

Figure 7 shows Raman spectra on isobaric heating of HDA at ~1.2 GPa (path 3′). The changes in the spectral features are basically similar to those at 0.6 GPa (Fig. 3), but the increase in relative intensity of the ~3400 cm^{-1} band is less pronounced compared to that observed at 0.6 GPa. In isothermally decompressing HDA obtained in path 3′ at 160 K and 1.2 GPa, we expect similar drastic changes in the Raman spectra as seen in the results of path 3. However, before capturing these possible changes we find that HDA crystallized (perhaps as ice II) at 0.4–0.5 GPa without showing the above transitions.

On the other hand, further isobaric heating of HDA at 1.2 GPa leads to crystallization of ices VI and XII above 170–180 K, as discussed below (Sec. III B). It is interesting to note that the formation of distinct crystalline ice phases upon heating HDA at similar *P-T* conditions have been reported,[32,33] though the phases have not been identified by diffraction. Klotz *et al.*[34] have shown that HDA systematically transforms (crystallizes) on heating at 0.3–3.9 GPa. They concluded that HDA crystallizes to high temperature proton-disordered structures found adjacent to the melting line of water at similar densities, though the thermodynamically stable phases at the crystallization temperatures are phases II, IX, VI, and VIII (all are proton ordered except for ice VI). For example, at 0.5–0.7 GPa mixtures of ices IV and V with a minor amount of ice XII formed at ~175 K upon heating HDA. According to their explanation, these similarities in the crystallization of HDA and liquid water under pressure arise from their origin in common structural features of the disordered systems at variable densities. Additionally, there is a heating rate dependence of the ice formation.[26] Their relative yields depend in a systematic manner on the heating rate. Further, Salzmann *et al.*[35] recently reported a detailed study of crystallization kinetics starting from HDA and its relation to heating rate and pressure. Both the effects of heating rate and pressure on the crystallization kinetics can be used to form desired ice phases (parallel reaction). As the type of ice formed also depends on the *P-T* conditions, the crystallization kinetics thus becomes more complicated at low temperatures and these moderately high pressures.

The VHDA phase that forms at 1.15 GPa on isobaric heating of HDA up to ~160 K has been proposed to be an additional distinct form of amorphous water.[4] The density of VHDA is reported to be higher than HDA by about 9%. The pressure dependence of the Raman spectrum of VHDA apparently has not been reported, though Loerting *et al.*[4] re-

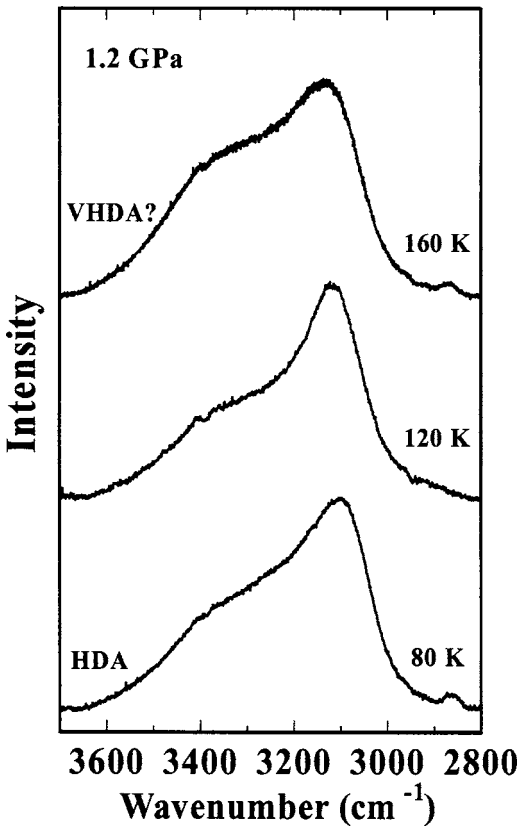

FIG. 7. HDA probed by *in situ* Raman spectroscopy in the region of the OH stretching bands as a function of temperature near ~1.2 GPa (path 3′).

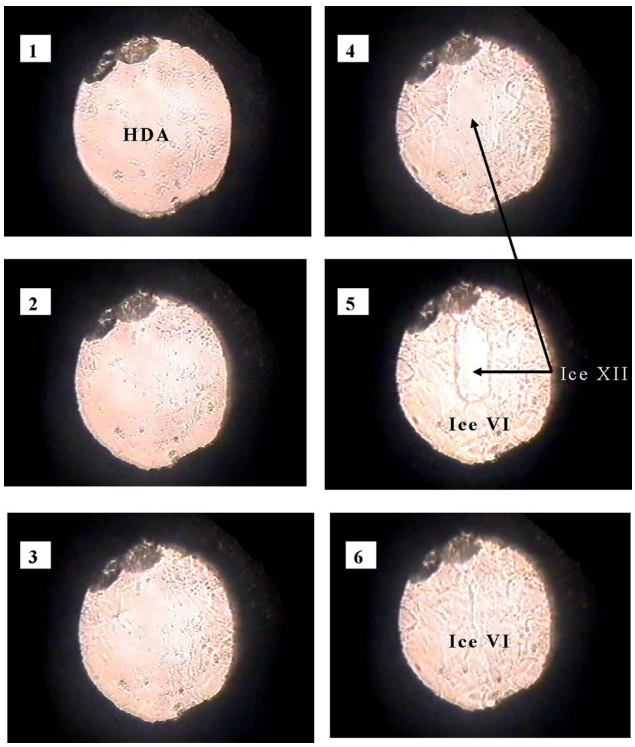

FIG. 8. (Color online) Photomicrographs showing the transition from HDA to ice XII, then finally to ice VI. The *P-T* conditions were ~1.25 GPa and 158–168 K, and the time evolution is about 15 min. Ice XII is the clear rectangle portion of images 4 and 5. Upon further heating complete crystallization to ice VI occurred, as shown in image 6.

ported the Raman spectrum of VHDA at normal pressure conditions. The formation conditions for the phase suggest that the spectrum at 160 K in our experiments (Fig. 7) corresponds to that of VHDA. The spectral features with temperature may arise from structural changes in VHDA, one and two molecules in close proximity of a first shell of hydrogen-bonded tetrahedral cage.[36] The possible relationship between VHDA and metastable fluid water is not clear. In particular, it is not known whether VHDA is a distinct phase, separated from HDA by a first-order transition, or whether it is simply densified HDA.

If we continue to compress HDA at ~135 K, the phase transforms to ice VII′ at about 3 GPa, as reported previously.[37] Ice VII′ is a crystalline phase close in structure to orientationally disordered ice VII.[1] As mentioned in the introduction, Loerting *et al.*[7] reported the LDA→HDA →VHDA transformation sequence near ~125 K. On compressing HDA isothermally, HDA transformed to VHDA at ~1.2 GPa. At a lower temperature (i.e., 100 K), the transformation does not appear to take place, and at a higher temperature of 150 K LDA crystallizes.[1] On decompressing VHDA isothermally at 135 K, LDA can be recovered at ambient pressure.[7] It is further claimed that in principle both the HDA and VHDA, and LDA and HDA transformations are reversible, though they are difficult to observe directly, probably due to the different activation energies. Although LDA and HDA can be converted into each other by compression or decompression (e.g., Fig. 5), our earlier study found evidence that ice VII′ also transforms to LDA on release of pressure to ambient pressure at 135 K.[37]

B. HDA→ice XII transition

Both ices XII and IV can form from liquid water in the stability field of ice V. They also form from HDA in the field of ice VI, and are metastable in both domains. Kohl *et al.*[21] showed that pure ices IV and XII can be formed in a reproducible manner on controlled isobaric heating of HDA. The key parameter in their preparation is the heating rate, with slow rates of ~0.5 K/min favoring formation of ice IV, whereas heating rates greater than ~15 K/min (e.g., shock heating) lead to the formation of ice XII. Ice XII is metastable with respect to ice V, and transformation of ice VI to ice XII is not evident in dielectric studies.[38]

Ice XII could be obtained on isobaric heating of HDA at 1.2–1.3 GPa (i.e., path 3′) by the procedure described by Kohl *et al.*[21] Photomicrographs showing the changes of a representative sample are shown in Fig. 8. Ice XII began to grow as a small region within HDA; upon further heating complete crystallization to ice VI occurred. We checked that the phase is identical to ice XII by x-ray diffraction.[39] Its x-ray pattern is consistent with that reported previously.[18,19] Ice VI could be obtained either directly from HDA or from ice XII on subsequent heating. We measured *in situ* Raman spectra on ice XII with temperatures and pressures ranging from 80 to 300 K and 0–3 GPa, respectively. Since ice XII phase can be quenched at various pressures and temperatures, a study such as this would be useful in improving the understanding of the phase boundaries of ice XII as a result of a detailed spectroscopic study of the high-pressure polymorphs in its real regions of stability. Figure 9 shows the

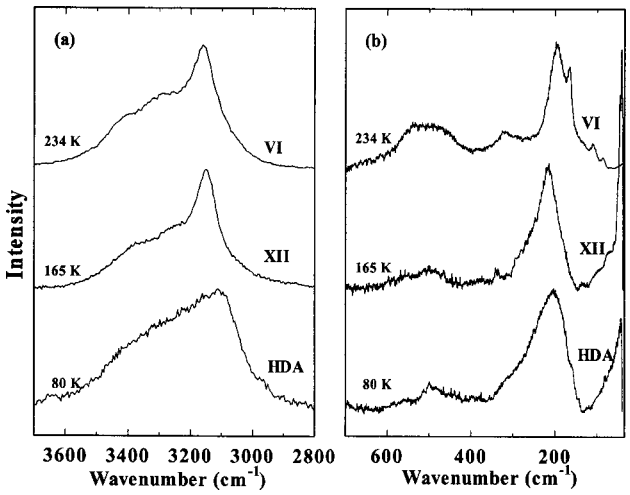

FIG. 9. *In situ* Raman spectra following the transition from ice I_h to HDA and ice XII as a function of temperature at ~1.2 GPa. (a) OH stretching region; (b) low frequency lattice vibration region.

representative OH stretching and low frequency spectra corresponding to the HDA→XII→VI transition sequence (path 3′). Once ice VI and/or ice XII were/was obtained, we again cooled the samples to 77 K and then either released pressure or applied further pressure to the sample.

The strongest Raman peaks in ice XII at various *P-T* conditions are shown in Fig. 10 together with the data corresponding to the phase reported by Chou *et al.*[24] and ice XII from Salzmann *et al.*[25] The frequencies of ices VI and XII are close, though the bands have different line shapes, especially in the low frequency region (Fig. 9). Ice VI is tetragonal $[P4_2/nmc]$,[40,41] and there are two separate interpenetrating networks linked through the four equatorial water molecules in hexamer units. Whereas, ice XII forms a tetragonal crystal $[I\bar{4}2d]$,[2] and contains a screw-type hydrogen-bonded arrangement with the smallest ring size consisting of seven and eight molecules.[3]

IV. DISCUSSION

In this section, we compare and discuss the results for metastable phases of H_2O obtained on various *P-T* paths starting with HDA. It is interesting to discuss our results in the context of the phase behavior of amorphous ice phases together with a proposed liquid-liquid phase transition hypothesis and the relationships between recently observed metastable phases of ice within the stability region of ice VI.

Recent diffraction results have been interpreted in terms of a continuous conversion of HDA to LDA.[42] Those conclusions are based on experimental conditions within the annealing limits of HDA and do not agree with subsequent Raman studies.[43] Our results support the conclusions in Ref. 43 that conversions of HDA to LDA and/or LDA to HDA are discontinuous (Fig. 5).

The properties of a glass can be strongly affected by its thermal history. Since the properties of a nonergodic state depend upon the *P-T* path used to reach the state, it is expected that amorphization even at closely similar conditions may not lead to an identical state;[44] that is, T_g does not correspond strictly to isoviscosity conditions and depends on the heating rate and sample history. Thus, HDA produced by different pressure, temperature, and time (*P-T-t*) conditions would have a different T_g. More careful and controlled studies may be needed to produce their glassy states and to determine their T_g. X-ray[45] and neutron[46,47] diffraction measurements indicate that the structure of HDA is similar to that of liquid water at higher temperature and high pressure in the sense that the water molecules appear to be more independent and uncorrelated. Assuming a close similarity in structure between HDA and HDL, our results provide evidence that HDA has a structure similar to that of high-pressure liquid water.

HDA, like other amorphous phases produced from a crystalline phase on compression rather than by cooling from the liquid state, is not a glass in the conventional sense.[33,48,49] Accordingly, relaxation of HDA (e.g., by annealing) may be needed before its glass transition can be realized. We propose that the narrowing of the stretching band around 120 K (Fig. 7) is an indication of this relaxation. If the pressure is released to a proper value, the resultant HDA ice can relax more easily. Relaxation to the glassy state becomes faster when pressure is decreased at a fixed temperature (e.g., paths 2 and 3). This relaxation and glass transition phenomenon are kinetically controlled processes. Therefore, HDA samples recovered at 77 K and ambient pressure are metastable and readily convert to stable phases quickly so that the glass transition in HDA is difficult to observe.

Another interesting point concerns the T_g of LDA. Qualitative comparisons of DSC (differential scanning calo-

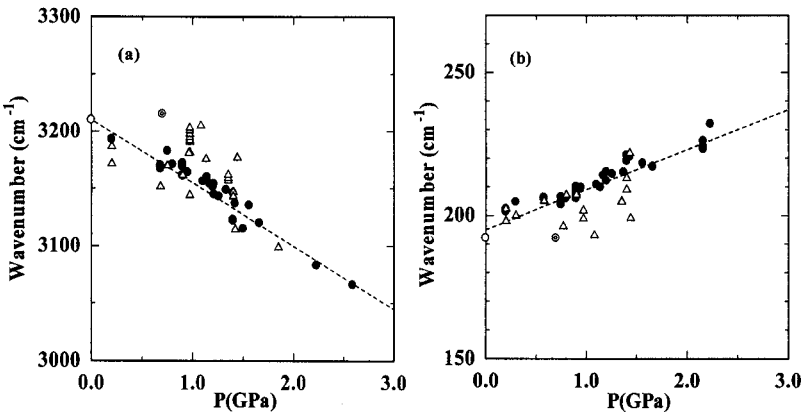

FIG. 10. Pressure dependences of the (a) OH stretching and (b) low frequency lattice mode frequencies at various temperatures. ●: ice XII, △: ice VI, ⊙: phase reported by Chou *et al.* (Ref. 24), ○: ice XII from Salzmann *et al.* (Ref. 25). The dotted line is a least-square fit of our ice XII data.

rimetry) scans against those of unrelated hyperquenched glasses have recently led to the conclusion that its T_g is 165 K instead of 136 K.[50] At the presumed glass transition temperature of 135 K, no relaxation processes can be detected on the time scale t of <4 ns.[51] It has been concluded based on high-resolution neutron backscattering measurements that LDA starts to crystallize into ice I_c at $T_g=135$ K, i.e., at the originally proposed T_g. On the other hand, self-diffusion studies have shown that following this path water is liquid at 150–160 K,[52] consistent with early diamond-anvil cell observations.[53] Experiments using a blunted conical indentor show that LDA formed from HDA behaves like viscous liquid near 143 K, much before its rapid crystallization to cubic ice.[54] Clearly, different kinetic behavior depends on sample history.[55–58]

It is useful to examine our results within the context of the liquid-liquid phase transition hypothesis. However, in doing so, we must state that the assumption that amorphous ice and supercooled liquid water are related remains to be established. As Raman spectra of LDL and HDL have not apparently been previously reported, a mere comparison of Raman bands does not allow the distinction between liquid and amorphous states. On the other hand, the phases obtained were very fragile (unstable) and it was not easy to maintain them in the cell for a long time. We needed to change pressure very delicately; otherwise the phase easily returned to "original" LDA and HDA mixed phases or crystallized which appears more "stable" at the same *P-T* condition. We tried to hold the phase obtained at ~145 K for a while, but the sample in the cell began to crystallize slowly after less than half an hour. Therefore, we speculate that the observations shown in Fig. 6 show the different structural transition behaviors in between Figs. 3 and 5.

The existence and location of the second C_p' within the *P-T* phase diagram of pure water are not yet clear. A number of theoretical calculations have been able to reproduce the liquid-liquid phase transition. The location of C_p' depends on the chosen effective potentials of water and shows variability. As an example, a C_p' at about 0.1 GPa and a temperature of 220 K has been proposed[59] (Fig. 1). Theoretical studies estimate that the location of the liquid-liquid critical point is below the homogeneous nucleation temperature (T_H). Thus, the critical point is thus difficult to probe experimentally with searching wide *P-T* areas because of rapid crystallization of pure bulk water. Mishima and Stanley[59] reported indirect evidence that the melting curve of ice IV using emulsified samples shows a sharp inflection in slope at the proposed line of the liquid-liquid transition. They stated that the results imply that ice IV melts into two different liquids (possibly HDL and LDL phases), and the HDL and LDL might coexist.

The results obtained in our study can be interpreted in terms of the existence of a second C_p' around 0.2–0.3 GPa and between T_H and T_X. Indeed, Kanno and Miyata[60] recently reported indirect experimental evidence that the C_p' of water has $P_c'=200$ MPa and $145\ \text{K}<T_c'<175$ K. These were determined from differential thermal analysis experiments for homogeneous ice nucleation with pressure. Since the phase boundary of LDA-HDA also lies at 0.2–0.3 GPa and is almost independent of temperature, the boundary defines a structural change from a low-density to a high-density phase. The configuration of HDL has been described as being close to the local structure of ice VI or VII,[61] both having interpenetrating tetrahedral networks. In this connection, it is interesting to note that a similar attempt to correlate to a structural change from a low-pressure icelike structure, such as I_h, III, and V, to a high-pressure icelike structure such as VI, VII, and VIII has been done recently.[62]

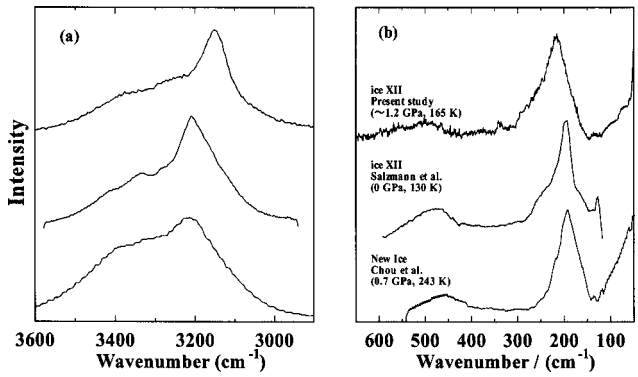

FIG. 11. Comparison of the Raman spectra of the present study, a new high-pressure phase of H_2O reported by Chou *et al.* (Ref. 24) and ice XII reported by Salzmann *et al.* (Refs. 25 and 63) (a) OH stretching region and (b) low frequency lattice mode region.

The same year that Lobban *et al.*[2] identified ice XII, Chou *et al.*[24] reported a new phase of ice that could be produced in the stability field of VI, specifically at 0.7–1.2 GPa and near melting temperatures of between 276 and 299 K. They speculated that the new phase may be related to a disordered anisotropic structure with some similarities to ice VI in view of the Raman spectra and crystal morphology. Subsequently, comparing Raman spectra, Salzmann *et al.*[25] proposed that the phase reported by Chou *et al.*[24] is ice XII. We discuss this proposal and the *P-T* regions in which ice XII is observed.

Salzmann *et al.*[25] published the Raman spectrum of pure ice XII. Though detailed assignment of the full Raman spectrum in ice XII requires further study, it is interesting that the low frequency region of ice XII also shows a broad peak with relatively high intensity at ~470 cm^{-1} in the librational region similar to HDA (and a sharp peak at 190 cm^{-1}; Fig. 11). The comparison of the spectra is shown in Fig. 11. The proposal that phase in Ref. 24 is ice XII was made on the basis of the close similarity in spectral features of the lower frequency of the phases. A weak peak in the low frequency Raman spectrum of ice XII having a frequency of 127 cm^{-1} was observed to be close to the band observed by Chou *et al.* at 123 cm^{-1},[63] although there are major differences in temperature [130 K (Ref. 25) and 243 K (Ref. 24)] and the overall band shape and resolution of the shoulders of OH stretching band region spectra between them are not comparable. As Salzmann *et al.*[25] pointed out, the comparison should be made under the same conditions. The remarkable point is that the peak data for the new ice clearly deviate from those for ice XII, by approximately +30 cm^{-1} in the OH stretching region and approximately −10 cm^{-1} in the lower frequency region as shown in Fig. 10. The conclusion we draw from

these peak data is that the phase reported in Ref. 24 is probably not ice XII. Thus, the question about the origin of the phase still remains open. However, we find that the frequencies of ice VI and the metastable phase of ice are close (Fig. 10). Moreover, the new ice phase has a density similar to that of ice VI,[24] the phase may be related to ice VI in the way that ice VII and ice VII′ formed by pressure-induced transformation of HDA shared similarities.[1]

The specific *P-T* range in which ice XII appears is not known, nor is the difference between the states in samples obtained by freezing the liquid at high pressures in the stability field of ice V, and by heating HDA from pressure-induced (amorphized) ice I_h. Koza *et al.*[24] stated that once ice XII is formed, it can persist up to at least 2 GPa at 77 K. We found that ice XII is still stable at higher pressures up to 3 GPa at ~77 K and 2.7 GPa at 100 K. This is consistent with the results reported by Klotz *et al.*[64] Ice polymorphs may coexist as a result of thermoelastic stability.[38] In the present work, we stress that there was no indication for the transformation from ice VI to ice XII at ~1 GPa over 158–212 K range. Therefore, the present data give direct experimental evidence that the Gibb's energy of ice XII is much higher than that of ice. VI at 1.1 GPa (e.g., Johari[38]).

V. CONCLUSIONS

I*n situ* high-pressure, low temperature techniques can be used to study metastable H_2O in previously inaccessible regimes. Raman spectra obtained under these conditions suggest the different phase behaviors that are distinct from that documented previously between LDA and HDA, which can occur at similar *P-T* conditions. Remarkable changes in the Raman line shapes were observed. The transition is reversible, and it appears to be rapid and sharp; there is no evidence for an intermediate phase, and the results strongly depend on *P-T* path. Comparison of the strongest Raman peak in ice XII with that of the metastable phase of ice originally found to form within the stability field of ice VI indicates that the phase is probably not ice XII. Thus, continued study is needed for unambiguous identification of the phase. Further experiments using these *in situ* methods should prove useful in detailing the anomalous behavior of water at low temperatures and its proposed liquid-liquid transition.

ACKNOWLEDGMENTS

The authors thank H. Kanno for useful discussions and V. V. Struzhkin and E. Gregoryanz for experimental assistance. This work was supported by NASA-NAI (NNG05GJ74G), NSF-DMR (0508988), and Carnegie/Department of Energy Alliance Center (CDAC-DE-FC03-03NA00144).

[1] R. J. Hemley, L. C. Chen, and H. K. Mao, Nature (London) **338**, 638 (1989).
[2] C. Lobban, J. L. Finney, and W. F. Kuhs, Nature (London) **391**, 268 (1998).
[3] M. O'Keeffe, Nature (London) **392**, 879 (1998).
[4] T. Loerting, C. Salzmann, I. Kohl, E. Mayer, and A. Hallbrucker, Phys. Chem. Chem. Phys. **3**, 5355 (2001).
[5] Y. Yoshimura, S. T. Stewart, M. Somayazulu, H. K. Mao, and R. J. Hemley, J. Chem. Phys. **124**, 024502 (2006).
[6] C. G. Salzmann, P. G. Radaelli, A. Hallbrucker, E. Mayer, and J. L. Finney, Science **311**, 1758 (2006).
[7] T. Loerting, W. Schustereder, K. Winkel, C. G. Salzmann, I. Kohl, and E. Mayer, Phys. Rev. Lett. **96**, 25702 (2006); T. Loerting, C. G. Salzmann, K. Winkel, and E. Mayer, Phys. Chem. Chem. Phys. **8**, 2810 (2006).
[8] O. Mishima and H. E. Stanley, Nature (London) **396**, 329 (1998).
[9] P. H. Poole, F. Sciortino, U. Essmann, and H. E. Stanley, Nature (London) **360**, 324 (1992).
[10] C. A. Angell, in *Water: A Comprehensive Treatise*, edited by F. Franks (Plenum, New York, 1982), Vol. 7.
[11] O. Mishima, J. Chem. Phys. **121**, 3161 (2004).
[12] A. Hallbrucker, E. Mayer, and G. P. Johari, J. Phys. Chem. **93**, 7751 (1989).
[13] G. P. Johari, A. Hallbrucker, and E. Mayer, J. Phys. Chem. **94**, 1212 (1990).
[14] H. Kanno and C. A. Angell, J. Chem. Phys. **73**, 1940 (1980).
[15] O. Mishima, J. Chem. Phys. **100**, 5910 (1994).
[16] Y. Katayama, T. Mizutani, W. Utsumi, O. Shimomura, M. Yamakata, and K. Funakoshi, Nature (London) **403**, 170 (2000).
[17] O. Ohtaka, H. Arima, H. Fukui, W. Utsumi, Y. Katayama, and A. Yoshiasa, Phys. Rev. Lett. **92**, 15506 (2004).
[18] M. Koza, S. Helmut, A. Tolle, F. Fujara, and T. Hansen, Nature (London) **397**, 660 (2000).
[19] M. M. Koza, H. Schober, T. Hansen, A. Tolle, and F. Fujara, Phys. Rev. Lett. **84**, 4112 (2000).
[20] C. G. Salzmann, T. Loerting, I. Kohl, E. Mayer, and A. Hallbrucker, J. Phys. Chem. B **106**, 5587 (2002).
[21] I. Kohl, E. Mayer, and A. Hallbrucker, Phys. Chem. Chem. Phys. **3**, 602 (2001).
[22] C. A. Tulk and D. D. Klug, Phys. Rev. B **63**, 212201 (2001).
[23] I. Kohl, E. Mayer, and A. Hallbrucker, J. Phys. Chem. B **104**, 12102 (2000).
[24] I.-M. Chou, J. G. Blank, A. F. Goncharov, H.-K. Mao, and R. J. Hemley, Science **281**, 809 (1998).
[25] C. G. Salzmann, I. Kohl, T. Loerting, E. Mayer, and A. Hallbrucker, J. Phys. Chem. B **106**, 1 (2002).
[26] T. Loerting, I. Kohl, C. Salzmann, E. Mayer, and A. Hallbrucker, J. Chem. Phys. **116**, 3171 (2002).
[27] J. C. Chervin, B. Canny, M. Guthier, and Ph. Pruzan, Rev. Sci. Instrum. **64**, 203 (1993).
[28] H. K. Mao, P. M. Bell, J. W. Shaner, and D. J. Steinberg, J. Appl. Phys. **49**, 3276 (1978); H. K. Mao, J. Xu, and P. M. Bell, J. Geophys. Res. **91**, 4673 (1986).
[29] O. Mishima, L. D. Calvert, and E. Whalley, Nature (London) **310**, 393 (1984).
[30] G. E. Walrafen, W.-H. Yang, and Y. Chu, in *Supercooled Liquids: Advances and Novel Applications*, edited by J. T. Fourkas, D. Kivelson, U. Mohanty, and K. A. Nelson (ACS, Washington, DC, 1997), Chap. 21.
[31] O. Mishima, L. D. Calvert, and E. Whalley, Nature (London) **314**, 76 (1985).
[32] O. Andersson, G. P. Johari, and H. Suga, J. Chem. Phys. **120**, 9612 (2004).
[33] Y. Yoshimura and H. Kanno, Chem. Phys. Lett. **349**, 51 (2001).
[34] S. Klotz, G. Hamel, J. S. Loveday, R. J. Nelmes, and M. Guthrie, Z. Kristallogr. **218**, 117 (2003).
[35] C. G. Salzmann, E. Mayer, and A. Hallbrucker, Phys. Chem. Chem. Phys. **6**, 5156 (2004).
[36] J. L. Finney, D. T. Brown, A. K. Soper, T. Loerting, E. Mayer, and A. Hallbrucker, Phys. Rev. Lett. **89**, 205503 (2002).
[37] Y. Yoshimura, H. K. Mao, and R. J. Hemley, Chem. Phys. Lett. **420**, 503 (2006).
[38] G. P. Johari, J. Chem. Phys. **118**, 242 (2003).
[39] Y. Yoshimura, S. T. Stewart, M. Somayazulu, H. K. Mao, and R. J. Hemley (unpublished).
[40] B. Kamb, Science **150**, 205 (1965).
[41] W. F. Kuhs, J. L. Finney, C. Vettier, and D. V. Bliss, J. Chem. Phys. **81**, 3612 (1984).
[42] C. A. Tulk, C. J. Benmore, J. Urquidi, D. D. Klug, J. Neuefeind, B. Tombeli, and P. A. Egelstaff, Science **297**, 1320 (2002).
[43] O. Mishima and Y. Suzuki, Nature (London) **419**, 599 (2002).
[44] O. Anderson and G. P. Johari, J. Chem. Phys. **121**, 3936 (2004).
[45] L. Bosio, G. P. Johari, and J. Teixeira, Phys. Rev. Lett. **56**, 460 (1986).
[46] M. A. Floriano, E. Whalley, E. C. Svensson, and V. F. Sears, Phys. Rev. Lett. **57**, 3062 (1986).

[47] M.-C. Bellissent-Funel and J. Teixeira, J. Chem. Phys. **87**, 2231 (1987).
[48] J. S. Tse, D. D. Klug, C. A. Tulk, I. Swainson, E. C. Svenson, C.-K. Loong, V. Shapakov, V. R. Belosludov, R. V. Beloslufov, and Y. Kawazoe, Nature (London) **400**, 647 (1999).
[49] J. S. Tse, J. Chem. Phys. **96**, 5482 (1992).
[50] V. Velikov, S. Borick, and C. A. Angell, Science **294**, 2335 (2001).
[51] M. M. Koza, G. Geil, H. Schober, and F. Natali, Phys. Chem. Chem. Phys. **7**, 1423 (2005).
[52] G. P. Johari, J. Chem. Phys. **22**, 36101 (2005).
[53] R. J. Hemley, The H_2O system under extreme conditions, 2nd International Workshop on Water Dynamics (Sendai International Center, Tohoku University, Sendai, Japan, November 11–12, 2004).
[54] G. P. Johari, J. Phys. Chem. B **102**, 4711 (1998).
[55] A. Minoguchi, R. Richert, and C. A. Angell, Phys. Rev. Lett. **93**, 215703 (2004).
[56] S. Cerveny, A. S. Gustavo, R. Bergman, and J. Swenson, Phys. Rev. Lett. **93**, 245702 (2004).
[57] R. Souda, Phys. Rev. Lett. **93**, 235502 (2004).
[58] G. P. Johari, J. Phys. Chem. B **107**, 9063 (2003).
[59] O. Mishima and H. E. Stanley, Nature (London) **392**, 164 (1998).
[60] H. Kanno and K. Miyata, Chem. Phys. Lett. **422**, 507 (2006).
[61] M. Canpolat, F. W. Star, A. Scala, M. R. Sadr-Lahijany, O. Mishima, S. Havlin, and H. E. Stanley, Chem. Phys. Lett. **294**, 9 (1998).
[62] T. Kawamoto, S. Ochiai, and H. Kagi, J. Chem. Phys. **120**, 5867 (2004).
[63] C. G. Salzmann, I. Kohl, T. Loerting, E. Mayer, and A. Hallbrucker, Phys. Chem. Chem. Phys. **6**, 1269 (2004).
[64] S. Klotz, G. Hamel, J. S. Loveday, M. Guthrie, and R. J. Nelmes, ISIS Rutherford Appleton Laboratory Report No. 11642, 2000–2001 (unpublished); http://www.isis.rl.ac.uk/isis2001/reports/11642.